RNAscope® Publications with the HALO® Image Analysis Platform

RNAscope® image analysis with the HALO® image analysis platform continues to advance research areas as diverse as immunology and infectious disease, metabolism, neuroscience, as well as oncology and immuno-oncology. RNAscope assays encompass *in situ* hybridization (ISH), fluorescence *in situ* hybridization (FISH), and codetection assays with an immunohistochemistry (IHC) or immunofluorescence (IF) component, such as ISH-IHC and FISH-IF. Here we list recent publications according to research area and highlight publications using ISH, FISH, and codetection assays using HALO image analysis. **Each citation is listed under the RNAscope modules used in each publication. Although many publications could have been placed into several categories, they are only listed once. Check any related categories for additional publications in your research area.**

Immunology & Infectious Disease

ISH & FISH

Harper J, Gordon S, Chan CN et al. CTLA-4 and PD-1 dual blockade induces SIV reactivation without control of rebound after antiretroviral therapy interruption. *Nat Med* **26**: 519-528 (2020). DOI: 10.1038/s41591-020-0782-y

ISH

McBrien JB, Mavigner M, Franchitti L et al. Robust and persistent reactivation of SIV and HIV by N-803 and depletion of CD8+ cells. *Nature* **578**: 154-159 (2020). DOI: 10.1038/s41586-020-1946-0

Mitigation of endemic GI-tract pathogen-mediated inflammation through development of multimodal treatment regimen and its impact on SIV acquisition in rhesus macaques

Authors: Bochart RM, Busman-Sahay K, Bondoc S, Morrow DW, Ortiz AM, Fennessey CM, Fischer MB, Shiel O, Swanson T, Shriver-Munsch CM, Crank HB, Armantrout KM, Barber-Axthelm AM, Langner C, Moats CR, Labriola CS, MacAllister R, Axthelm MK, Brenchley JM, Keele BF, Estes JD, Hansen SG, Smedley JV

Source: https://journals.plos.org/plospathogens/article/authors?id=10.1371/journal.ppat.1009565

Modification: Cropped

License: CCO 4.0, https://creativecommons.org/publicdomain/zero/1.0/

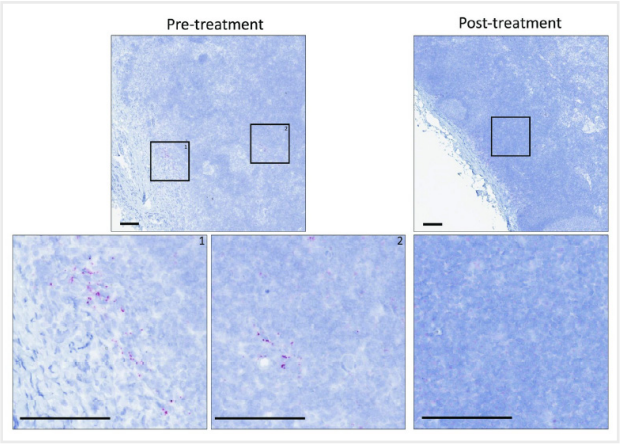

Science: Rachele Bochart and colleagues evaluate the impact of a short course multimodal therapy to eliminate common endemic macaque pathogens on the microbiome of the GI track in healthy macaques and evaluate the impact on acquisition of simian immunodeficiency virus (SIV). Treatment with a cocktail containing four drugs resulted in a stronger colonic mucosal barrier, reduced inflammation, and a more consistent rate of SIV infection, demonstrating a reproducible research model for analysis of SIV infection.

Technology: The HALO ISH module was used to detect 16sRNA as a proportion of total lymph node tissue (area/μm^2). Image analysis was performed on annotation layers drawn manually in HALO. In the figure shown above, RNAscope was performed on animals that showed colonic or peripheral inflammation by other biomarkers in order to quantify translocated bacteria using 16s rRNA probes in mesenteric lymph node tissue. Following treatment using a multimodal therapy containing four drugs to eliminate common macaque endemic pathogens, a reduction in 16s rRNA was observed, consistent with the epithelial barrier being restored.

ISH

Okoye AA, Duell DD, Fukazawa Y et *al*. CD8+ T cells fail to limit SIV reactivation following ART withdrawal until after viral amplification. *J Clin Invest* **131**: e141677 (2021). DOI: 10.1172/JCI141677

Schaut RG, Palmer MV, Boggiatto PM et *al*. Mucosal IFNγ production and potential role in protection in *Escherichia coli* O157:H7 vaccinated and challenged cattle. *Sci Rep* **11**: 9769 (2021). DOI: 10.1038/s41598-021-89113-7

Webb GM, Molden J, Bushman-Sahay K et *al*. The human IL-15 superagonist N-803 promotes migration of virus-specific CD8+ T and NK cells to B cell follicles but does not reverse latency in ART-suppressed, SHIV-infected macaques. *PloS Pathog* **16**: e1008339 (2020). DOI: 10.1371/journal.ppat.1008339

FISH

Schuler BA, Habermann AC, Plosa EJ et *al*. Age-determined expression of priming protease TMPRSS2 and localization of SARS-CoV-2 infection in the lung epithelium. *J Clin Invest* **131**: e140766 (2020). DOI: 10.1172/JCI140766

Wang Y, Lifschitz L, Gellatly K et *al*. HIV-1-induced cytokines deplete homeostatic innate lymphoid cells and expand TCF7-dependent memory NK cells. *Nat Immunol* **21**: 274-286 (2020). DOI: 10.1038/s41590-020-0593-9

Metabolism

ISH & FISH

Adriaenssens AE, Biggs EK, Darwish T et *al*. Glucose-Dependent Insulinotropic Polypeptide Receptor-Expressing Cells in the Hypothalamus Regulate Food Intake. *Cell Metab* **30**: 987-996.e6 (2019). DOI: 10.1016/j.cmet.2019.07.013

ISH

Bird TG, Müller M, Boulter L et *al*. TGFβ inhibition restores a regenerative response in acute liver injury by suppressing paracrine senescence. *Sci Transl Med* **10**: eaan1230 (2018). DOI: 10.1126/scitranslmed.aan1230

Cavino K, Sung B, Su Q et *al*. Glucagon Receptor Inhibition Reduces Hyperammonemia and Lethality in Male Mice with Urea Cycle Disorder. *Endocrinology* **162**: bqaa211 (2020). DOI: 10.1210/endocr/bqaa211

Nyborg NCB, Kirk RK, de Boer AS et *al*. Cholecystokinin-1 receptor agonist induced pathological findings in the exocrine pancreas of non-human primates. *Toxicol Appl Pharm* **399**: 115035 (2020). DOI: 10.1016/j.taap.2020.115035

FISH

Brandt C, Nolte H, Henschke S et *al*. Food Perception Primes Hepatic ER Homeostasis via Melanocortin-Dependent Control of mTOR Activation. *Cell* **175**: 1321-1335.e20 (2018). DOI: 10.1016/j.cell.2018.10.015

Gutierrez GD, Xin Y, Okamoto H et *al*. Gene Signature of Proliferating Human Pancreatic α-Cells. *Endocrinology* **159**: 3177-3186 (2018). DOI: 10.1210/en.2018-00469

Ruud LE, Pereira MMA, de Solis AJ et *al*. NPY mediates the rapid feeding and glucose metabolism regulatory functions of AgRP neurons. *Nat Commun* **11**: 1-12 (2020). DOI: 10.1038/s41467-020-14291-3

ISH-IHC

Bentsen MA, Rausch DM, Mirzadeh Z et *al*. Transcriptomic analysis links diverse hypothalamic cell types to fibroblast growth factor 1-induced sustained diabetes remission. *Nat Commun* **11**: 4458 (2020). DOI: 10.1038/s41467-020-17720-5

Neuroscience

ISH

Johnson MA, Contoreggi NH, Kogan JF et *al*. Chronic stress differentially alters mRNA expression of opioid peptides and receptors in the dorsal hippocampus of female and male rats. *J Comp Neurol* **529**: 2636-2657 (2021). DOI: 10.1002/cne.25115

Orexin receptors 1 and 2 in serotonergic neurons differentially regulate peripheral glucose metabolism in obesity

Authors: Xiao X, Yeghiazaryan G, Hess S, Klemm P, Sieben A, Kleinridders A, Morgan DA, Wunderlich FT, Rahmouni K, Kong D, Scammell TE, Lowell BB, Kloppenburg P, Brüning JC, Hausen AC

Source: https://www.nature.com/articles/s41467-021-25380-2

Modification: Cropped

License: CC BY 4.0, https://creativecommons.org/licenses/by/4.0/

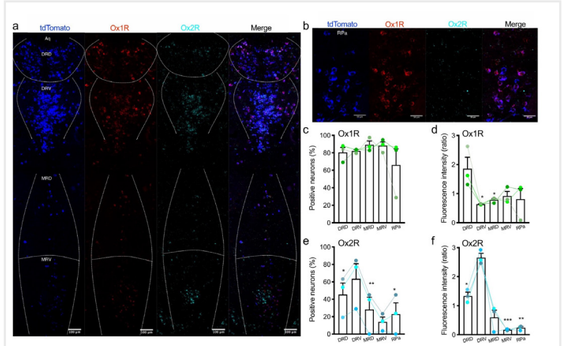

Science: Orexin receptors play a critical role in glucose homeostasis. Xiao and colleagues demonstrate differential localization and functional roles of orexin receptors 1 and 2 in serotonergic neurons. Specifically, with respect to functional roles in mice with diet-induced obesity, they find that inactivation of the type 1 orexin receptor in the serotonin transporter expressing cells led to reduced insulin sensitivity via decreasing glucose utilization in brown fat and skeletal muscle, while inactivation of the type 2 receptor improved insulin sensitivity by a decrease in gluconeogenesis in the liver. Future research on this pathway may lead to therapies for obesity.

Technology: HALO image analysis was used to characterize distribution and quantify the endogenous expression of Ox1R and Ox2R in the dorsal (DRD), ventral (DRV), and median raphe nucleus (dorsal MRD, ventral MRV) of a $SERT^{tdTomato}$ mouse using RNAscope FISH in (a) shown above. In (b), RNAscope FISH is shown in the raphe pallidus. In (c) and (e), percentages of Ox1R and Ox2R positive neurons is shown. In (d) and (f), the average relative fluorescence intensity of Ox1R or Ox2R signal is shown in each type of serotonergic neuron. While Ox1R is expressed in the majority of tdTomato positive serotonergic neurons throughout the raphe nucleus, Ox2R was expressed at lower levels with expression peaking in the DRV.

Functionally distinct POMC-expressing neuron subpopulations in hypothalamus revealed by intersectional targeting

Authors: Biglari N, Gaziano I, Schumacher J, Radermacher J, Paeger L, Klemm P, Chen W, Corneliussen S, Wunderlich CM, Sue M, Vollmar S, Klöckener T, Sotelo-Hitschfeld T, Abbasloo A, Edenhofer F, Reimann F, Gribble FM, Fenselau H, Kloppenburg P, Wunderlich FT, Brüning JC

Source: https://www.nature.com/articles/s41593-021-00854-0

Modification: Cropped

License: CC BY 4.0, https://creativecommons.org/licenses/by/4.0/

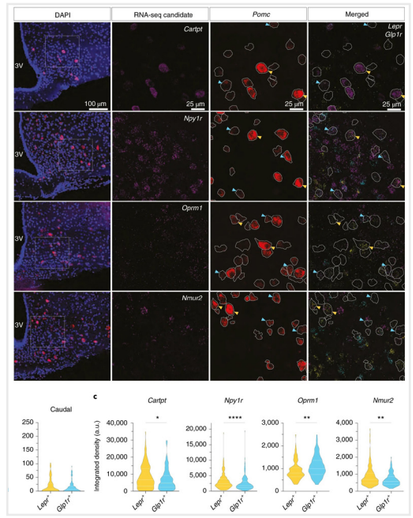

Science: Nasim Biglari and colleagues set out to understand the heterogeneity of pro-opiomelanocortin (POMC)-expressing neurons in the hypothalamus which are important regulators of metabolic homeostasis. Using new mouse models to examine POMC neurons expressing the leptin receptor (*Lepr*) and glucagon like peptide 1 receptor (*Glp1r*) they demonstrate that $POMC^{Lepr+}$ and $POMC^{Glpr1+}$ neurons have unique localization patterns in the hypothalamus, have distinct electrophysiological properties, and differential ability to suppress feeding. They further investigate translational signatures of these neuron subtypes and identify differentially expressed genes for further characterization. Insights from this publication and from future studies using the mouse models published here may lead to the ability to modulate metabolic signaling in the hypothalamus.

Technology: Images were captured on a Leica confocal TCS SP-8-X microscope and maximum intensity projections were created. The FISH module of HALO was used to quantify expression of *Lepr*, *Glp1r*, and *Pomc* along with candidate genes identified from ribotag enrichment experiments and RNAseq, *Cartpt*, *Npy1r*, *Oprm1*, and *Nmur2* in mice of 12 weeks of age in the arcuate nucleus of the hypothalamus. In the figure shown above, *Pomc*-positive neurons are annotated in white, while yellow arrows indicate *Lepr*-positive neurons and cyan arrows represent *Glp1r*-positive POMC neurons. Violin plots quantify FISH signal. This experiment validated previous RNAseq experiments by confirming differential expression of *Cartpt*, *Npy1r*, *Oprm1*, and *Nmur2* in $POMC^{Lepr+}$ and $POMC^{Glpr1+}$ neurons.

FISH

Guitierrez-Mecinas M, Bell AM, Shepherd F *et al*. Expression of cholecystokinin by neurons in mouse spinal dorsal horn. *J Comp Neurol* **527**: 1857-1871 (2019). DOI: 10.1002/cne.24657

Hishimoto A, Pletnikova O, Lang DL *et al*. Neurexin 3 transmembrane and soluble isoform expression and splicing haplotype are associated with neuron inflammasome and Alzheimer's disease. *Alzheimers Res Ther* **11**: 28 (2019). DOI: 10.1186/s13195-019-0475-2

Jolly S, Lang V, Koelzer VH *et al*. Single-Cell Quantification of mRNA Expression in The Human Brain. *Sci Rep* **9**: 12353 (2019). DOI: 10.1038/s41598-019-48787-w

Ruud J, Alber J, Tokarska A *et al*. The Fat Mass and Obesity-Associated Protein (FTO) Regulates Locomotor Responses to Novelty via D2R Medium Spiny Neurons. *Cell Rep* **27**: 3182-3198.e9 (2019). DOI: 10.1016/j.celrep.2019.05.037

Saucisse N, Mazier W, Simon V *et al*. Functional heterogeneity of POMC neurons relies on mTORC1 signaling. *Cell Rep* **37**: 109800 (2021). DOI: 10.1016/j.celrep.2021.109800

Oncology & Immuno-Oncology

ISH

Duncan DJ, Scott M, Scorer P *et al*. Assessment of PD-L1 mRNA and protein expression in non-small cell lung cancer, head and neck squamous cell carcinoma and urothelial carcinoma tissue specimens using RNAScope and immunohistochemistry. *PloS One* **14**: e0215393 (2019). DOI: 10.1371/journal.pone.0215393

Galbraith LCA, Mui E, Nixon C *et al*. PPAR-gamma induced AKT3 expression increases levels of mitochondrial biogenesis driving prostate cancer. *Oncogene* **40**: 2355-2366 (2021). DOI: 10.1038/s41388-021-01707-7

Hesterberg AB, Rios BL, Wolf EM *et al*. A distinct repertoire of cancer-associated fibroblasts is enriched in cribriform prostate cancer. *J Pathol Clin Res* **7**: 271-286 (2021). DOI: 10.1002/cjp2.205

Hornburg M, Desbois M, Lu S *et al*. Single-cell dissection of cellular components and interactions shaping the tumor immune phenotypes in ovarian cancer. *Cancer Cell* **39**: 928-944.e6 (2021). DOI: 10.1016/j.ccell.2021.04.004

Hu H, Piotrowska Z, Hare PJ *et al*. Three subtypes of lung cancer fibroblasts define distinct therapeutic paradigms. *Cancer Cell* **39**: 1531-1547.e10 (2021). DOI: 10.1016/j.ccell.2021.09.003

Najumudeen AK, Ceteci F, Fey SK *et al*. The amino acid transporter SLC7A5 is required for efficient growth of KRAS-mutant colorectal cancer. *Nat Genet* **53**: 16-26 (2021). DOI: 1038/s41588-020-00753-3

Newman AC, Falcone M, Uribe AH *et al*. Immune-regulated IDO1-dependent tryptophan metabolism is source of one-carbon units for pancreatic cancer and stellate cells. *Mol Cell* **81**: 2290-2302.e7 (2021). DOI: 10.1016/j.molcel.2021.03.019

FISH

Chen H-C, Eling N, Martinez-Jimenez CP *et al*. IL-7-dependent compositional changes within the γδ T cell pool in lymph nodes during ageing lead to an unbalanced anti-tumour response. *Embo Rep* **20**: e47379 (2019). DOI: 10.15252/embr.201847379

Jiang H, Liu X, Knolhoff BL *et al*. Development of resistance to FAK inhibition in pancreatic cancer is linked to stromal depletion. *Gut* **69**: 122-132 (2020). DOI: 10.1136/gutjnl-2018-317424

FISH-IF

Pelka K, Hofree M, Chen JH *et al*. Spatially organized multicellular immune hubs in human colorectal cancer. *Cell* **184**: 4734-4752 (2021). DOI: 10.1016/j.cell.2021.08.003

ISH-IHC

Siersbæk R, Scabia V, Nagarajan S, *et al*. IL6/STAT3 signaling hijacks estrogen receptor α enhancers to drive breast cancer metastasis. *Cancer Cell* **38**: 412-423 (2020). DOI: 10.1016/j.ccell.2020.06.007

Other

ISH

Guo L, Wang Z, Anderson CM *et al*. Ultrasensitive automated RNA in situ hybridization for kappa and lambda light chain mRNA detects B-cell clonality in tissue biopsies with performance comparable or superior to flow cytometry. *Modern Pathol* **31**: 385-394 (2018). DOI: 10.1038/modpathol.2017.142

Breast and pancreatic cancer interrupt IRF8-dependent dendritic cell development to overcome immune surveillance

Authors: Meyer MA, Baer JM, Knolhoff BL, Nywening TM, Panni RZ, Su X, Weilbaecher KN, Hawkins WG, Ma C, Fields RC, Linehan DC, Challen GA, Faccio R, Aft RL, DeNardo DG

Source: https://www.nature.com/articles/s41467-018-03600-6

Modification: Cropped

License: CC BY 4.0, https://creativecommons.org/licenses/by/4.0/

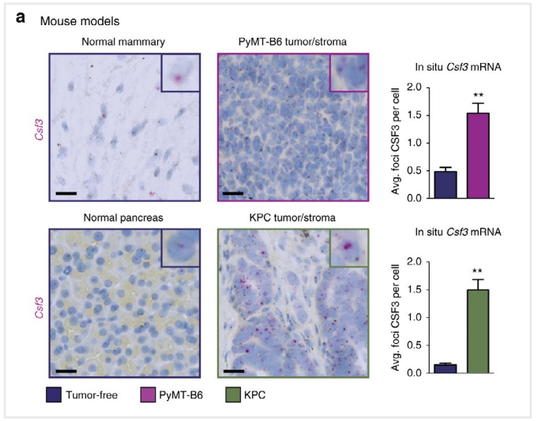

Science: Meyer and colleagues identify a new mechanism by which tumors subvert anti-tumor immunity by disrupting differentiation of conventional dendritic cells (cDC). They investigate cDC and bone marrow progenitors of cDC in human and mouse models of breast and pancreatic cancers and find systemic decreases in the cDC1 subset and their progenitors. This finding is clinically relevant as poor patient outcomes are associated with reductions in cDC1 development that impair CD8+ T-cell responses.

Technology: Whole slide tissue scans imaged at 20x were analyzed with the ISH module of HALO. As Meyer and colleagues found upregulation of granulocyte colony-stimulating factor (GCSF) in the blood of tumor bearing mice relative to tumor-free controls, they next examined expression of the ligand of the GCSF receptor, *Csf3*, using ISH. Shown in (a) above, ISH for *Csf3* is performed on normal mammary tissue and on end-stage PyMT-B6 mice, as well as normal pancreatic tissue and KPC tumor tissue. Quantification demonstrates an increase in expression in *Csf3* in both mouse models for breast and pancreatic cancer.

Age-associated expression of p21 and p53 during human wound healing

Authors: Chia CW, Sherman-Baust CA, Larson SA, Pandey R, Withers R, Karikkineth AC, Zukley LM, Campisi J, Egan JM, Sen R, Ferrucci L

Source: https://onlinelibrary.wiley.com/doi/10.1111/acel.13354

Modification: Cropped

License: CC BY 4.0, https://creativecommons.org/licenses/by/4.0/

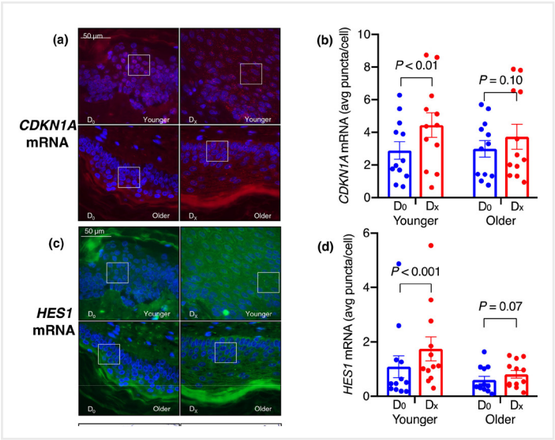

Science: Chee Chia and colleagues investigated the expression of p16, p21 and additional biomarkers associated with senescence in a wound healing study with two cohorts in order to examine an age effect. A biopsy punch created the wound and established baseline expression, and a second concentric biopsy punch was acquired several days later for expression analysis using IHC and RNAscope. This research group found that p21 and p53 were induced specifically in younger subjects, suggesting that human cutaneous wound healing can be characterized by age and expression of the p21 and p53 biomarkers.

Technology: Cyclin Dependent Kinase Inhibitor 1A (*CDKN1A*) expression was examined as it is a gene strongly associated with senescence and in regeneration of damaged or missing tissue in mice. Quantification of a FISH RNAscope assay by the FISH module of the HALO image analysis software revealed an increase in *CDKN1A* mRNA in younger subjects (a, b) shown above D_0 indicates baseline and D_x indicates the wound sample. To determine if *CDKN1A* activation occurred via Notch activation, *HES1*, a Notch target gene was assessed (c). Quantification of *HES* mRNA by HALO (d) revealed a significant increase in younger wound subjects.

Todorović V, Su Z, Putman CB *et al*. Small Molecule IL-36γ Antagonist as a Novel Therapeutic Approach for Plaque Psoriasis. *Sci Rep* **9**: 9089 (2019). DOI: 10.1038/s41598-019-45626-w

For More Information

Visit https://learn.indicalab.com/literature to view all of our customer publications. To learn more about the RNAscope image analysis in HALO, download the Quantitative RNAscope™ Image Analysis Guide and visit the following HALO module webpages: ISH, FISH, ISH-IHC, and FISH-IF.

About Indica Labs

Indica Labs is the world's leading provider of computational pathology software and image analysis services. Our flagship HALO® and HALO AI™ platform facilitates quantitative evaluation of digital pathology images. HALO Link™ facilitates research-focused image management and collaboration while HALO AP® enables collaborative clinical case review.

Through a combination of precision, performance, scalability, and usability our software solutions enable pharmaceutical companies, diagnostic labs, research organizations, and Indica's own contract pharma services team to advance tissue-based research, clinical trials, and diagnostics.

HALO® HALO LINK® PHARMA SERVICES powered by indica labs HALO AI® HALO AP®

Contact us for more information, demo, or trial.

US Headquarters

Indica Labs, Inc
8700 Education Pl NW, Bldg B
Albuquerque, NM 87114 USA
+1 (505) 492-0979
info@indicalab.com

UK and Europe

+44 (0)1789 765 721
emea@indicalab.com

Japan

+81 (0)70 4180 7730)
japan@indicalab.com

China

+86 13761896143
china@indicalab.com

Tech Support: support@indicalab.com
Website: https://indicalab.com

indica-labs @Indicalab

indica labs